# COMPUTATIONS OF WIND STRESS FIELDS OVER THE ATLANTIC OCEAN

S. HELLERMAN

U.S. Weather Bureau, Washington, D.C.

ABSTRACT

A review is made of the procedures used by the Scripps Institute of Oceanography and by Hidaka in the first systematic attempts to compute the field of mean wind stress, $\bar{\tau}$, over the oceans by means of the resistance law. $\bar{\tau}$ over the Atlantic is then recomputed using the more detailed wind speed frequency data that have become available since the Scripps and Hidaka computations. For this purpose two procedures are used, similar to the method used by Scripps for the North Atlantic, but designed to take advantage of the finer grouping of the data. In consideration of the effects of the wind stress field on the wind-driven circulation, the results indicate essentially no significant differences in the $\bar{\tau}$-fields from the various procedures. However, the $\bar{\tau}$-field varies considerably with the several rather different neutral stability evaluations of drag coefficient, $C_D^N$. Depending upon which of the various determinations of $C_D^N$ is used in the resistance law, the forcing function for the wind-driven permanent currents may easily vary by a factor of two.

## 1. INTRODUCTION

Most theoretical models concerned with the analysis of the permanent ocean currents recognize that such currents are largely forced by the curl of the stress of the mean annual winds, $\nabla\times\bar{\tau}$, on the sea surface. From a linear version of the vorticity equation Sverdrup [13] derived a simple equation for mass transport, integrated from the surface to the bottom.

$$\beta\frac{\partial\psi}{\partial x}=\nabla\times\bar{\tau} \qquad (1)$$

where

$$\nabla\times\bar{\tau}=\frac{\partial\tau_y}{\partial x}-\frac{\partial\tau_x}{\partial y}$$

$\beta$ is the $y$-derivative of the Coriolis parameter; $\psi$ is the mass transport streamfunction; $x$ and $y$ are the coordinates in the eastern and northern directions respectively; and $\tau_x$ and $\tau_y$ are the $x$ and $y$ components of the wind stress in the sea surface respectively. Sverdrup was able to explain many features of the observed current of the eastern part of the North Pacific as a consequence of this simple equation. With this important role of the $\nabla\times\bar{\tau}$-field in mind the Scripps Institute of Oceanography [11] undertook the first systematic computations of $\bar{\tau}$ over the North Pacific Ocean, and this work was extended by Scripps [12] to the North Atlantic and by Hidaka [5] to the Indian and Southern Hemisphere Oceans.

Wind-rose data for the Scripps Pacific and the Hidaka computations contained only a mean wind speed from each direction, and relative frequency of direction. For the Atlantic computations wind data were available that contained wind speed frequency from each direction, though two of the speed categories were rather broad; Beaufort numbers 1, 2, and 3 were lumped together into a single category and Beaufort numbers 5 and 6 into another. Data for the broad oceans and for long time periods have since become available in speed categories from which rather good estimates of relative frequencies of winds in each Beaufort interval can be made. One object of this study is to re-examine the Atlantic $\bar{\tau}$-field when evaluated from this finer grouping of wind speed data.

A second purpose for this study is to obtain some quantitative measure of the limits between which the $\bar{\tau}$-field may vary with what is certainly one of the more uncertain elements in its evaluation, the drag coffiecient, $C_D^N$. (The superscript $N$ indicates that the drag coefficients are determined under neutral stability conditions.)

## 2. REVIEW

The mean annual stress, $\bar{\tau}$, in all cases is computed from a form of the resistance law, wherein stress on the sea is independent of the stability of the atmosphere in the first few meters above the sea.

$$\tau_0=\rho C_D^N u_a^2 \qquad (2)$$

$\tau_0$ is the stress of the wind on the sea surface in the direction of the wind observed at leval $a$; $C_D^N$ represents the drag coefficient for neutral stability conditions; $\rho$ is the air density immediately above the sea surface; and $u_a$ is the wind speed at "anemometer height" $a$. From here on subscripts 0 and $a$ will be omitted. This study assumes, with Scripps and Hidaka, that the broad ocean $\bar{\tau}$-fields are appropriately approximated from $C_D^N$, i.e., that the effect of stability on the effective stress is small. But there is still considerable scatter even in the various determinations of $C_D^N$ [17]. The $\tau$-field will therefore be evaluated with the $C_D^N$ used by Scripps and Hidaka, as well as with the $C_D^N$ of more recent measurements, where $C_D^N$ is a function of $u$ alone.

For their North Pacific computations Scripps used U.S. Hydrographic Pilot Chart wind data and the resistance law, equation (2). Pilot chart wind-roses group data by months and in 5° quadrilaterals, and give only mean wind speed from each direction, with no indication of the frequency distribution about the mean. It was therefore necessary for Scripps to approximate these distributions (a) with the aid of U.S Weather Bureau [16] for middle and high latitudes and (b) with normal distribution functions [8] for lower latitudes.

When the $\bar{\tau}$-field for the Atlantic was computed, Scripps had available wind data classified by speed on U.S. Weather Bureau "Summary of Marine Data" (SMD) cards and in the "Monthly Meteorological Charts of Atlantic" (MM Charts) of the British Air Ministry. SMD cards contain speed data in Beaufort Number (BN) categories shown in table 1.

SMD cards were used almost exclusively for the North Atlantic and MM Charts were used mainly south of 5°S. MM Charts contain relative frequency data for speed intervals $i=3$ and $i=4$ separately, while SMD cards lump BN 4, 5, 6 together.

By direct application of (2)

$$\tau_j=\frac{\sum_i \rho(C_D^N)_i f_{i,j} u_i^2}{\sum_i f_{i,j}}$$

$\tau_j$ is the component of stress from the $j$th direction, and $f_{i,j}$ is the relative frequency in the $i$th speed interval. $\rho$ is a climatological value of air density at sea level. Scripps used the drag coefficients, $(C_D^N)_i$, of the early determinations of Rossby and Montgomery [10], Rossby [9], and Montgomery [6], which indicated a sudden transition at the critical wind speed of 6.7 m. sec.$^{-1}$ of surface roughness, hence of $C_D^N$.

$$(C_D^N)_i=\begin{cases}0.0008, & u_i<6.7 \text{ m. sec.}^{-1}\\ 0.0017, & u_i=6.7 \text{ m. sec.}^{-1}\\ 0.0026, & u_i>6.7 \text{ m. sec.}^{-1}\end{cases} \quad (3)$$

## 3. EFFECTS OF COMPUTATION PROCEDURES

In this study the Scripps Atlantic procedure was somewhat modified to take advantage of the additional wind data of two volumes of the U.S. Navy [14], [15] atlas. $\bar{\tau}$ was also calculated by approximating the classed wind speed data of these Navy volumes with continuous frequency distribution curves. Both of these procedures are described in the Appendix. An example of the effect of the method of computation and data grouping on resultant $|\bar{\tau}|$, using the Navy's climatological data and $C_D^N$ of equation (3), is shown in table 2 for an ocean area centered on 17.1° N., 56.3° W.

To simplify comparison of the broad $\nabla\times\bar{\tau}$-fields it is convenient to use as a basis for comparison the quantity $\nabla\times\bar{\tau}/\beta$, integrated from eastern shore to western shore along latitude lines. From equation (1) this quantity is understood to have physical meaning in the sense that it is an approximation to the total wind-driven meridional mass transport at each latitude. The negative of this quantity, from continuity considerations, is then an approximation of the intensity of the western boundary current.

Table 3 shows that the mean annual western boundary current computed from the Scripps Atlantic (col. 2), the modified Scripps Atlantic (col. 3), and the continuous frequency procedures (col. 4) are very nearly the same. It seems reasonable, therefore, to assume that the Scripps Atlantic procedure, which used the coarsest grouping of data of the three, is at least sufficient for computing the mean annual $\nabla\times\bar{\tau}$-field, especially in view of the much larger variations of the western boundary current from other uncertainties.

TABLE 1.—*Beaufort categories of wind speed data on SMD cards.*

| Interval ($i$) | Beaufort number (BN) | Range (m. sec.$^{-1}$) | Mean speed ($u_i$) |
|---|---|---|---|
| 1 | 0 | 0 - 0.3 | 0 |
| 2 | 1, 2, 3 | 0.4- 5.4 | 2.9 |
| 3 | *4 | 5.5- 7.9 | 6.7 |
| 4 | *5, 6 | 8.0-13.8 | 10.9 |
| 5 | 7 | 13.9-17.1 | 15.5 |
| 6 | 8 | 17.2-20.7 | 19.0 |
| 7 | 9- | 20.8- | 22.6 |

*Approximated from the broader class BN 4, 5, and 6 with the aid of MM charts.

## 4. DRAG COEFFICIENTS

In spite of the intense efforts that have been made in recent years to evaluate $C_D^N$ as a function of wind speed, this coefficient remains the most uncertain quantity in the evaluation of $\bar{\tau}$ by the resistance law. The mean annual western boundary current was therefore evaluated by the continuous frequency procedure for:

(a) The $C_D^N$ dependence on wind speed (Rossby and Montgomery [10]) given by equation (3) and used by Scripps and Hidaka.

(b) $C_D^N=(1.00+0.07\,u)\times10^{-3}$, in the range $0\leq u\leq 14$ m. sec.$^{-1}$ A survey by Deacon and Webb [3] of the values of

TABLE 2.—*Magnitude of the mean monthly stresses, $|\bar{\tau}|$, in dynes cm.$^{-2}$ at 17.1°N., 56.3° W.*

| | Scripps Pacific procedures | Modified Scripps Atlantic procedure | Continuous frequency procedure |
|---|---|---|---|
| January | 1.12 | 1.51 | 1.24 |
| February | .77 | 1.09 | 1.05 |
| March | .59 | .84 | .82 |
| April | .60 | .77 | .80 |
| May | .79 | 1.04 | 1.02 |
| June | 1.08 | 1.38 | 1.33 |
| July | 1.34 | 1.63 | 1.50 |
| August | .83 | 1.11 | 1.13 |
| September | .56 | .79 | .75 |
| October | .59 | .70 | .69 |
| November | .64 | .93 | .91 |
| December | .75 | 1.07 | 1.04 |

TABLE 3.—*Western boundary current (positive=northward) in $10^{12}$gm. sec.$^{-1}$ Sc. At.=Scripps Atlantic procedure. M. Sc. At.=modified Scripps Atlantic procedure. C. F.=continuous frequency procedure. M.=$C_D^N$ of equation (3). Sur.=$C_D^N$ of "Survey". D. H. =$C_D^N$ of the 2d Derwent Hunter trials. H. Err.=western boundary current error due to large error in gale $C_D^N$*

| (1) Lat. | (2) Sc. At. | (3) M. Sc. At. | (4) C. F. | (5) M | (6) Sur. | (7) D. H. | (8) H. Err. |
|---|---|---|---|---|---|---|---|
| 57.5°N. | −19.4 | −20.3 | −19.5 | −19.4 | −16.2 | −12.5 | ±2.6 |
| 52.5 | −7.4 | −8.4 | −7.8 | −7.4 | −6.4 | −4.9 | ±1.0 |
| 47.5 | 5.9 | 5.3 | 5.9 | 5.9 | 4.9 | 3.9 | ±1.0 |
| 42.5 | 14.2 | 13.8 | 14.1 | 14.2 | 11.7 | 9.1 | ±2.0 |
| 37.5 | 20.7 | 20.1 | 20.2 | 20.7 | 16.5 | 12.6 | ±2.1 |
| 32.5 | 27.2 | 26.2 | 25.9 | 27.2 | 20.6 | 15.6 | ±1.9 |
| 27.5 | 32.1 | 30.7 | 30.2 | 32.1 | 23.6 | 17.6 | ±1.5 |
| 22.5 | 22.4 | 21.0 | 20.8 | 22.4 | 15.9 | 11.8 | ±.7 |
| 17.5 | 12.3 | 11.0 | 10.9 | 12.3 | 8.2 | 6.0 | ±.1 |
| 12.5 | 1.5 | 1.0 | 1.0 | 1.5 | 0.8 | 0.7 | ±.1 |
| 7.5 | −4.6 | −4.5 | −4.6 | −4.6 | −3.3 | −2.3 | ±0.0 |
| 2.5 | 1.4 | 1.5 | 1.2 | 1.4 | 0.9 | 0.7 | ±.1 |
| 2.5°S. | 3.4 | 2.9 | 3.1 | 3.4 | 2.3 | 1.6 | ±.1 |
| 7.5 | 7.2 | 5.7 | 6.2 | 7.2 | 4.6 | 3.2 | ±.1 |
| 12.5 | .6 | .6 | −.1 | .6 | .3 | .1 | ±0.0 |
| 17.5 | −12.2 | −13.1 | −12.0 | −12.2 | −8.7 | −6.5 | ±.3 |
| 22.5 | −27.2 | −26.9 | −25.7 | −27.2 | −20.0 | −15.1 | ±1.4 |
| 27.5 | −36.7 | −34.1 | −33.9 | −36.7 | −27.8 | −21.2 | ±2.8 |
| 32.5 | −39.2 | −38.3 | −36.8 | −39.2 | −30.8 | −23.7 | ±4.2 |

$C_D^N$ determined in nine separate investigations suggested this regression line. Earlier, Munk [7], from a model proposed by Jeffries, concluded that one component of $\tau$ is proportional to $u^2$, and another to $u^3$, and that therefore $C_D^N$ should be a linear function of $u$.

(c) $C_D^N$ recently evaluated by Deacon [2] from data gathered in the second "Derwent Hunter" trials, for near neutral conditions, in the range 5–13 m. sec.$^{-1}$ These values represent, as well, determinations by Brocks [1] and Fleagle, Deardorff, and Badgley [4], all three evaluations of $C_D^N$ as functions of $u$ alone being in general agreement.

(d) The same as (c) except for winds of gale force. Gale $C_D^N$ were changed radically to simulate a large error in $C_D^N$, in this region where determinations of it are almost entirely lacking.

Figure 1 shows the four sets of $C_D^N$ for which western boundary currents were computed. Because of the difficulty of making accurate wind profile measurements when winds are of gale force and seas are high, $C_D^N$ in gales is virtually unknown, and it was therefore necessary to make subjective extrapolations out to 32 m. sec.$^{-1}$

Columns 5, 6, and 7 of table 3 give the western boundary currents in $10^{12}$ gm. sec.$^{-1}$ for the three rather different sets of $C_D^N$ and column 8 shows the possible error in the western boundary currents for the hypothetical error in the Derwent Hunter gale $C_D^N$ of figure 1. It is noteworthy that the permanent western boundary current may be different by as much as a factor of two, depending upon the $C_D^N$ used. Until there is sufficient evidence to favor one set of $C_D^N$ this sizeable uncertainty remains in the forcing function for a large-scale wind-driven ocean circulation.

As mentioned above, the results presented here are for $C_D$ determined under neutral or near neutral stability conditions, with the assumption that the mean annual

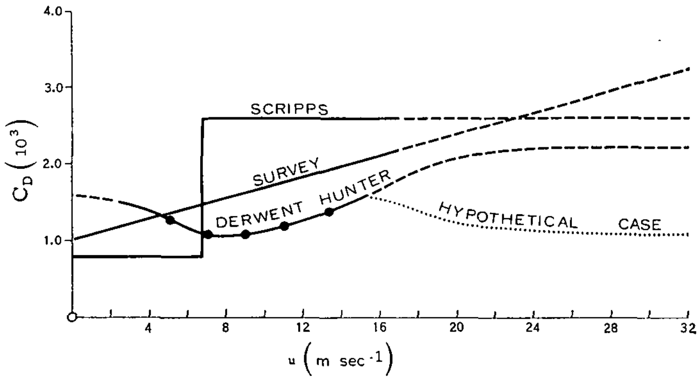


FIGURE 1.—Neutral stability drag coefficients as functions of wind speed, for which western boundary currents are tabulated in table 1.

western boundary current is little changed by the stability effect. There is observational evidence, however, that the effect of stability can be quite large locally, especially in cold air outbreaks over relatively warm seas. The U.S. Navy [14], [15] atlas shows large wintertime climatological air-sea temperature differences in a region roughly coincident with the narrow western boundary current. It is likely, therefore, that the effect of stability is an important perturbation influence that should not be neglected where the detail of the boundary current is to be investigated.

Figure 2 shows the mean monthly western boundary current for each month. The continuous frequency procedure and the Derwent Hunter $C_D^N$ were used. The salient feature here is the sudden increase in western boundary current intensity in late fall, in the region of 30° N., and the gradual decrease during most of the rest of the year to a minimum in early fall.

Figures 3 and 4 are maps of $\sum_j |\bar{\tau}_j|$, a quantity of interest in the study of dissipation of the winds by surface drag, for January and July respectively. The $j$ are the eight directions of the wind rose of the Navy atlas. Again, the continuous frequency procedure and the Derwent Hunter $C_D^N$ were used. The $C_D^N$ of equation (3) would increase these values roughly by 50–100 percent.

## APPENDIX

$\bar{\tau}$ was computed from U.S. Navy [14], [15] data for 75 "oceanographic areas" and coastal stations of the North and South Atlantic. Oceanographic areas consist first of all of fixed ocean stations wherever available. The bulk of the oceanographic areas, however, are small areas, roughly 28,000 to 38,000 mi.$^2$, representative of the "climatological" regions in which they appear, and selected largely along established trade routes. For such areas it is possible to obtain sufficient observations for the construction of frequency distributions. Wind frequency data appear in the following forms and categories.

Denote the relative frequency of winds from the $j$th

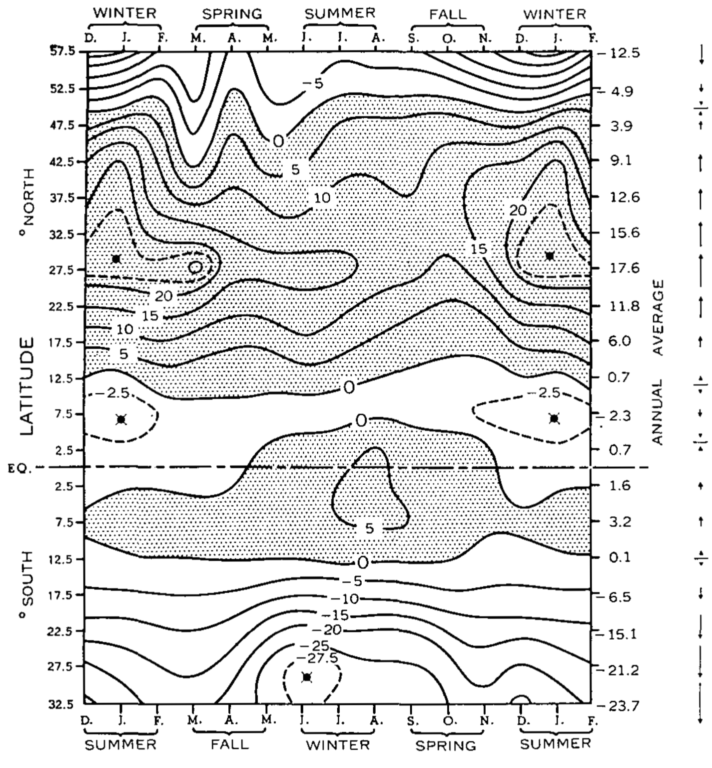


FIGURE 2.—Mean monthly western boundary currents in $10^{12}$ gm. sec.$^{-1}$ for each month of the year.

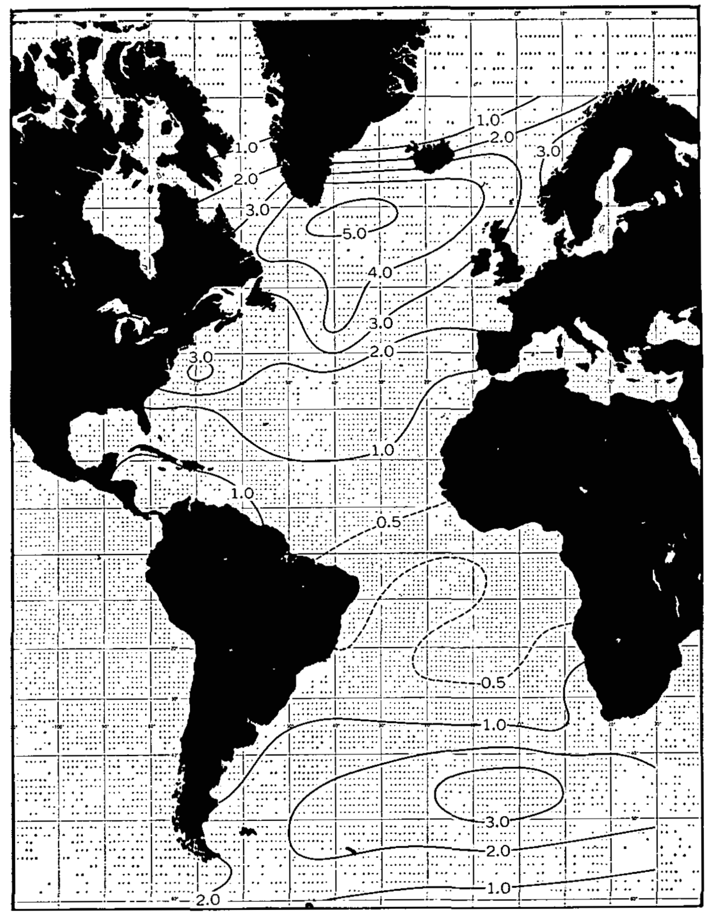


FIGURE 3.—$\sum_{j=1}^{8} |\bar{\tau}_j|$ in dynes cm.$^{-2}$ for January.

direction in Beaufort category $i$ by $f_{i,j}$, in Beaufort category $i+(i+1)$ by $f_{(i)\ (i+1),j}$ and denote wind frequencies from all directions combined in Beaufort category $i$ by $F_i$: for example, $f_{(4)(5),j}$ is the relative frequency of winds in the speed category including Beaufort numbers 4 and 5 from the $j$th direction; $F_5$ is the relative frequency of winds from all directions in the speed category Beaufort number 5. Then [14] and [15] provide the following relative frequency data:

$$f_{(2)(3),j};\ f_{(4)(5),j};\ f_{(6)(7),j};\ f_G=f_{(8)(9)(10)(11),j}$$

and

$$F_{(0)(1)};\ F_2;\ F_3;\ F_4;\ F_5;\ F_6;\ F_7;\ F_8;\ and\ F_9$$

In the following, the stress from an arbitrary direction $j$ is discussed and the direction subscript, $j$, will therefore be omitted (but understood).

For the Scripps Modified Atlantic procedure, wherever the Navy atlas data lumps two or more Beaufort categories together, i.e., for $f_{(2)(3)}$, $f_{(4)(5)}$, $f_{(6)(7)}$, and $f_G$, frequencies are apportioned between the individual Beaufort categories with the following assumptions. For $f_0$ through $f_7$,

$$F_0=F_1$$

$$f_i/f_{(i)(i+1)}=F_i/F_{(i)(i+1)},\ i=2,4,6$$

$$f_i/f_{(i)(i-1)}=F_i/F_{(i)(i-1)},\ i=3,5,7$$

$$f_1/f_2=F_1/F_2$$

To get $f_8$, $f_9$, $f_{10}$, and $f_{11}$, i.e., the relative frequency of winds in each Beaufort interval in the gale class, the following procedure is used.

The sum of gale frequencies from all directions is

$$F_G=\sum_{j=1}^{8}(f_G)_j$$

Then

$$F_{(10)(11)}=F_G-(F_8+F_9)$$

From a scatter diagram of $F_{(10)(11)}$ versus $F_G$, (regardless of season or geographical location) and a regression line drawn by eye

$$F_{(10)(11)}\approx F_G\approx 1/6$$

It is then assumed that

$$f_8/f_G=(5/6)(F_8/F_{(8)(9)})$$

$$f_9/f_G=(5/6)(F_9/F_{(8)(9)})$$

$$f_{10}/f_G=5/36$$

$$f_{11}/f_G=1/36$$

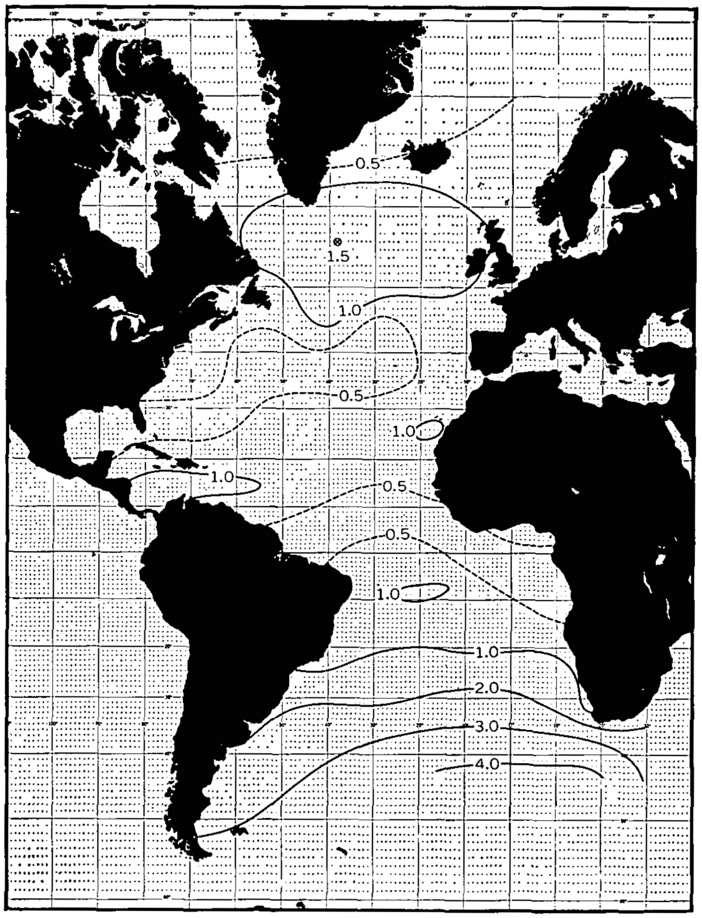


FIGURE 4.—$\sum_{j=1}^{8} |\bar{\tau}_j|$ in dynes cm.$^{-2}$ for July.

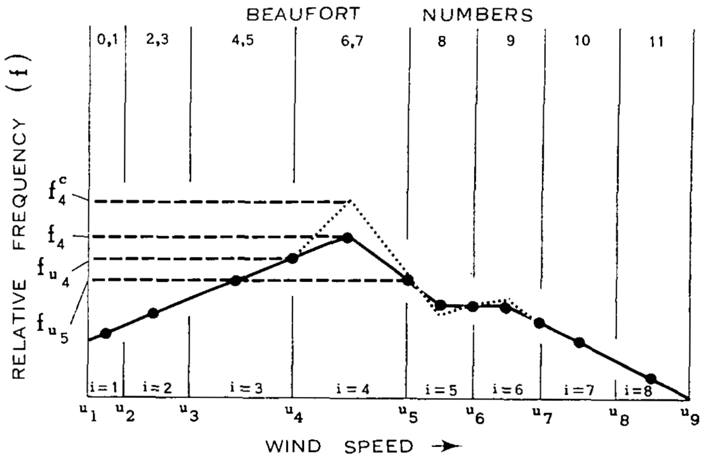


FIGURE 5.—Specimen of a relative frequency distribution of wind speeds. Dotted lines are the adjustments required to avoid violation of the given data.

The continuous frequency procedure assumes an $f$-distribution made up of straight line segments connecting $f_i$ at the center of each interval, $i$, as in figure 5. The $f$-distribution is then adjusted so that the observed mean $f_i$ for each interval is unchanged. Then

$$\tau=\sum_{i=1}^{N} \tau_i=\sum_{i=1}^{N} \rho \int_{u_i}^{u_{i+1}} C_D^N(u) g_i(u) u^2 du \tag{4}$$

$\tau$ is the stress from an arbitrary direction, $j$, $\tau_i$ is the stress contribution by the $i$th segment of the $f$-distribution curve; $u_i$ is the lower speed of the $i$th segment; $u_{i+1}$ is the higher speed of the $i$th segment; $g_i(u)=(f_{i+1}-f_i)(u_{i+1}-u_i)^{-1}(u-u_i)+f_i$; and $N=16$ (=number of straight-line segments).

$f_8, f_9, f_{10}$ and $f_{11}$ are determined in the same way as in the Modified Scripps method, and we get $f_{(0)(1)}$ from

$$f_{(0)(1)}/f_{(2)(3)}=F_{(0)(1)}/F_{(2)(3)}$$

All $f_i$ are normalized by divisions by the width of the Beaufort interval $u_{i+1}-u_i$.

The procedure for adjustment is as follows. The frequencies at interval extremes, $f_{u_i}$, are determined by linear interpolation for $i=2, \ldots, 8$, and for $i=1$ and $i=9$ by linear extrapolation. If $f_i=0$, the $f$'s at interval extremes are set equal to zero, $f_{u_i}=f_{u_{i+1}}=0$. The frequency at the center of the interval is then adjusted to $f_i^c$ (keeping all $f_{u_i}$ fixed) according to

$$f_{u_i}+2f_i^c+f_{u_{i+1}}=4f_i$$

i.e., so that frequency for each interval remains unchanged from that given by the Navy atlas. Figure 2 shows this type of adjustment in $i=4$, 5, and 6.

It is possible because of the last adjustment, that $f_i^c<0$. In this case $f_i^c$ is set equal to zero and $f_{u_i}$ and $f_{u_{i+1}}$ are changed to $f'_{u_i}$ and $f'_{u_{i+1}}$ respectively by

$$f'_{u_i}/f'_{u_{i+1}}=f_{u_i}/f_{u_{i+1}}$$

and

$$f'_{u_i}+f'_{u_{i+1}}=4f_i$$

The $f$-distribution is now completely described by a linear approximation to the original classed data of the Navy atlas. Equation (3) is then applied to obtain $\tau_j$, and the $\tau_j$ added vectorially to obtain $\tau_x$ and $\tau_y$.

## ACKNOWLEDGMENT

The writer gratefully acknowledges the encouragement and guidance received from Drs. K. Bryan, E. Kung, and S. Manabe, and the data-processing and programming assistance of Miss M. B. Jackson. Thanks are also due E. Rayfield for the drafting of the figures, and Mrs. R. A. Brittain and Miss J. K. Neal for assisting with the manuscript.

## REFERENCES

1. K. Brocks, "Measurement of Wind Profiles Over the Sea and the Drag at the Sea Surface," Paper presented at International Oceanographic Congress, New York, September 1959.
2. E. L. Deacon, "Aerodynamic Roughness of the Sea," *Journal of Geophysical Research*, vol. 67, No. 7, July 1962, pp. 3167–3172.

3. E. L. Deacon and E. K. Webb, "Small Scale Interactions," Sect. 2, pp. 43–87 in *The Sea*, vol. I, Interscience Publishers, New York, 1962.
4. R. G. Fleagle, J. W. Deardorff, and F. I. Badgley, "Vertical Distribution of Wind Speed, Temperature and Humidity Above a Water Surface," *Journal of Marine Research*, vol. 17, 1958, pp. 141–157.
5. K. Hidaka, "Computation of the Wind Stresses Over the Oceans," *Records of Oceanographic Works in Japan*, vol. 4, No. 2, Mar. 1958, pp. 77–123.
6. R. B. Montgomery, "Measurement of Vertical Gradient of Wind Over Water," *Papers in Physical Oceanography and Meteorology*, Massachusetts Institute of Technology and Woods Hole Oceanographic Institution, Part 2 of vol. 4, No. 3, 1936.
7. W. H. Munk, "Wind Stress on Water: an Hypothesis," *Quarterly Journal of the Royal Meteorological Society*, vol. 31, No. 349, July 1955, pp. 320–332.
8. R. O. Reid, "The Equatorial Currents of the Eastern Pacific as Maintained by the Wind," *Journal of Marine Research*, vol. 7, No. 3, 1948, pp. 1–101.
9. C.-G. Rossby, "On the Frictional Force Between Air and Water and On the Occurrence of a Laminar Boundary Layer Next to the Surface of the Sea," *Papers in Physical Oceanography and Meteorology*, Massachusetts Institute of Technology and Woods Hole Oceanographic Institution, Part 1 of vol. 4, No. 3, 1936.
10. C.-G. Rossby and R. B. Montgomery, "The Layer of Frictional Influence in Wind and Ocean Currents," *Papers in Physical Oceanography and Meteorology*, Massachusetts Institute of Technology and Woods Hole Oceanographic Institution, vol. 3, No. 3, 1935, 101 pp.
11. Scripps Institute of Oceanography, University of California, "The Field of Mean Wind Stress Over the North Pacific Ocean," *Oceanographic Report* No. 14 on Office of Naval Research Contract No. N60ri–111, Task Order VI, Sept. 1948.
12. Scripps Institute of Oceanography, University of California, "The Mean Wind Stress Over the Atlantic Ocean," *Oceanographic Report* No. 21 on Office of Naval Research Contract No. N60ri–111, Task Order VI, April, 1950.
13. H. U. Sverdrup, "Wind-Driven Currents in a Baroclinic Ocean; With Application to the Equatorial Currents of the Eastern Pacific," *Proceedings of the National Academy of Sciences*, vol. 33, No. 11, 1947, pp. 318–326.
14. U.S. Navy, Chief of Naval Operations, "Marine Climatic Atlas of the World, Vol. I, North Atlantic," NAVAER 5–1c–528, Washington, D.C., 1955.
15. U.S. Navy, Chief of Naval Operations, "Marine Climatic Atlas of the World, Vol. IV, South Atlantic," NAVAER 50–1c–531, Washington, D.C., 1958.
16. U.S. Weather Bureau, *Atlas of Climatic Charts of the Oceans*, Washington, D.C., 1958, 130 pp.
17. B. W. Wilson, "Note on Surface Wind Stress Over Water at Low and High Wind Speeds," *Journal of Geophysical Research*, vol. 65, No. 10, Oct. 1960, pp. 3377–3381.


*[Received September 1, 1964; revised December 16, 1964]*